Identification of a Disulfide Switch in BsSco, a Member of the Sco Family of Cytochrome *c* Oxidase Assembly Proteins[†,‡]

Qilu Ye,[§] Iveta Imriskova-Sosova,[§] Bruce C. Hill,* and Zongchao Jia

Department of Biochemistry, Queen's University, Kingston, Ontario K7L 3N6, Canada

Received September 9, 2004; Revised Manuscript Received November 24, 2004

ABSTRACT: BsSco is a membrane-associated protein from *Bacillus subtilis* characterized by the sequence CXXXCP, which is conserved in yeast and human mitochondrial Sco proteins, and their bacterial homologues. BsSco is involved in the assembly of the Cu_A center in cytochrome *c* oxidase and may play a role in the transfer of copper to this site. We have characterized the soluble domain of BsSco by biochemical, spectroscopic, and structural approaches. Soluble BsSco is monomeric in solution, and the two conserved cysteines are involved in an intramolecular cystine bridge. The cystine bridge is easily reduced, and circular dichroism spectroscopy shows no large-scale changes in BsSco's secondary structure upon reduction. The crystal structure of soluble BsSco, determined at 1.7 Å resolution, reveals typical elements of a thioredoxin fold. The CXXXCP motif, in which Cys45 and Cys49 are conserved, is located in a turn structure on the surface of the protein. In various native and His135Ala mutant structures, both disulfide-bonded and non-disulfide-bonded forms of CXXXCP are observed. However, despite extensive attempts, copper has not been found near or beyond the CXXXCP motif, a presumptive copper-binding site. Another potential copper binding residue, His135, is located in a highly flexible loop parallel to the CXXXCP loop but is more than 10 Å from Cys45 and Cys49. If these three residues are to coordinate copper, a conformational change is necessary. The structural identification of a disulfide switch demonstrates that BsSco has the capability to fill a redox role in Cu_A assembly.

The heme−copper oxidases of aerobic respiratory chains are oligomeric, integral membrane protein complexes. Perhaps the best-known members of the heme−copper family are the cytochrome *c* oxidases that act as terminal enzymes in respiratory chains of mitochondria and some aerobic bacteria. Cytochrome *c* oxidase catalyzes electron transfer from cytochrome *c* to molecular oxygen, giving water as the primary product and generating a proton electrochemical gradient (*1*). The multimeric structures of bacterial and mitochondrial enzymes are strikingly similar within the two core subunits (I and II) that are required for catalytic activity (*2*). These two subunits contain four redox active centers: two heme A moieties (i.e., cytochrome *a* and cytochrome a_3) and two copper centers (i.e., Cu_A and Cu_B). The assembly of cytochrome *c* oxidase is a multistep process depending on several accessory proteins responsible for the transport and insertion of heme and copper cofactors, as well as magnesium, zinc, and sodium ions, and for coordination of the assembly and folding of the subunits (*3*). Functional cytochrome *c* oxidase requires a total of three copper ions to be inserted into two centers. One center is a dinuclear copper site within the soluble domain of subunit II (i.e., Cu_A), and the second is a mononuclear site within subunit I (i.e., Cu_B) that is buried within the membrane (*2*). The mechanisms for how copper ions are delivered to Cu_A and Cu_B sites are poorly understood.

In the past few years, information about a new protein family, the Sco[1] family, has emerged (*4*). Proteins belonging to this family are required for the assembly of cytochrome *c* oxidase in both prokaryotic (*5*) and eukaryotic cells (*6*). Sco1 was first identified in yeast (*7*), and other members of this family have been recognized by the similarity of their sequence to that of Sco1. The key features of sequence similarity among Sco proteins are a pair of cysteine residues in the sequence CXXXCP and a histidine residue ∼84 amino acids toward the C-terminus. EXAFS studies with recombinant Sco1 from yeast have led to the proposal that the conserved cysteines and single histidine serve as inner sphere ligands for copper coordination (*8*).

In addition to the proposed copper binding and transfer functions of Sco1, it is also suggested, because of limited sequence similarity to bacterial thioredoxins, that Sco1 may

[†] This work is supported by grants from the Canadian Institutes of Health Research to Z.J. and B.C.H. and from the Canadian Foundation for Innovation to Protein Function Discovery Group. Z.J. is a Canada Research Chair in Structural Biology.

[‡] Protein Data Bank entry 1X2O.

* To whom correspondence should be addressed: Department of Biochemistry, Queen's University, Kingston, Ontario K7L 3N6, Canada. Telephone: (613) 533-6375. Fax: (613) 533-2497. E-mail: hillb@post.queensu.ca.

[§] These authors contributed equally to this work.

[1] Sco nomenclature: Sco, family of proteins implicated to play a role in cytochrome *c* oxidase assembly and recognized by their sequence similarity to the founding member, Sco1; Sco1, Sco family member from yeast, found as integral member of the inner mitochondrial membrane and known to play a role in Cu_A assembly; BsSco, Sco homologue found in *B. subtilis* anchored to the plasma membrane by a covalently attached diacylglyceride moiety; His-BsSco, recombinant form of native BsSco supplemented with a C-terminal hexahistidine tag and expressed as a membrane protein in *B. subtilis*; sBsSco, soluble domain of BsSco expressed in *E. coli* and in which the natural lipidation site has been removed; sBsScoHA, soluble BsSco in which His135 has been changed to Ala.

10.1021/bi0480537 CCC: $30.25
Published on Web 02/05/2005

act as a thiol:disulfide oxidoreductase (*9*). It is feasible that Sco1 may coordinate the reduction of cysteine residues, within the copper-binding center of subunit II of cytochrome *c* oxidase, with the insertion of copper. Efficient Cu_A assembly in yeast seems to require participation of at least one additional accessory protein, known as Cox17 (*10*). Yeast Cox17 is a 69-residue, water-soluble protein that is found in both the cytoplasm and mitochondrial intermembrane space (*11*). However, the strict requirement for Cox17 in this process is not supported by the lack of a homologue of Cox17 in *Bacillus subtilis*. In addition, the exclusive function of Sco in Cu_A assembly is questioned by the finding that some bacteria express an apparent Sco homologue but do not make a protein containing a Cu_A center (*12*). A more general function for Sco proteins in protection against oxidative stress is envisioned.

A member of the Sco family is expressed in the aerobic Gram-positive bacterium *B. subtilis* (i.e., BsSco) from the *ypmQ* gene. BsSco is required for the assembly of Cu_A, but not for the assembly of Cu_B (*13*). Hydropathy analysis of BsSco's sequence, derived from the sequence of the *ypmQ* gene, predicts that the first 20−24 amino acids make up a transmembrane α-helix. However, this sequence includes a signal peptidase II recognition site (*14*), and mass spectra of purified BsSco show that the mature protein is processed (*15*). Processing of native BsSco involves cleavage at cysteine residue 19 followed by attachment of a diacyl glycerol moiety to the thiol side chain of the now N-terminal cysteine residue. Mature, native BsSco is, therefore, anchored to the membrane via this covalently attached lipid.

Purification of wild-type BsSco or His-tagged, recombinant BsSco from *B. subtilis* plasma membranes yields only small amounts of protein (i.e., 0.1−0.5 mg/L) (*15*). In addition, expression of native, lipidated BsSco is lethal in *Escherichia coli*. Therefore, to obtain quantities of BsSco appropriate for biochemical and biophysical characterization, the soluble domain was expressed in *E. coli* as a fusion protein (*16*). Cleavage of the fusion protein gives a soluble version of BsSco (i.e., sBsSco) that is free of covalently bound lipid and has an additional two amino acids, relative to the native processed protein. We propose that sBsSco is a useful model of the membrane-anchored native protein. The two conserved cysteine residues are susceptible to oxidation, and in purified sBsSco, the vast majority is present as an intramolecular cystine bridge that can be easily reduced. Analysis of UV circular dichroism spectra shows that sBsSco is a mixture of α-helical and β-sheet secondary structural elements that is similar to that found for the lipid-bound protein isolated from *B. subtilis* plasma membranes. We have determined the sBsSco structure at 1.7 Å resolution. Numerous attempts have been made to generate crystals of copper-bound sBsSco without success. As our work was progressing, the solution structure of a similar construct of sBsSco was determined by NMR (*17*). These workers were also unable to obtain a structure for a copper−Sco complex, although evidence of copper binding was reported. Our findings extend this structural work, and in addition, we have observed oxidized and reduced forms of the protein involving formation and dissolution of a disulfide bond between the two conserved cysteine residues. The two redox states of sBsSco differ in their conformation in the vicinity of the cysteine-containing loop and in the loop containing the conserved His135; however, there is little change in sBsSco's overall structure. The facile redox activity of these two cysteines is consistent with a proposed function of Sco as a thioredoxin for the Cu_A site of subunit II.

EXPERIMENTAL PROCEDURES

Protein Expression, Purification, and Crystallization. Protein expression, purification, and crystallization of sBsSco were carried out as previously described (*16*). Briefly, the portion of *ypmQ* encoding the soluble domain of BsSco was cloned into the pGEX-4T3 expression vector, and transformed into *E. coli* DH5α cells for sBsSco expression, or into the methionine auxotroph DL41DE3 for Se-Met labeling. The recombinant proteins were overexpressed as fusion constructs with glutathione *S*-transferase and purified by affinity chromatography on glutathione−Sepharose 4 Fast Flow (Amersham). The His135Ala mutant of sBsSco, which was originally constructed for expression in *B. subtilis* (*13*), was amplified and transferred to the pGEX-4T3 expression vector and purified from *E. coli* in the same manner as native sBsSco. The purity of the preparations was checked routinely by electrophoresis in denaturing 15% polyacrylamide gels run under reducing conditions. The presence of copper in sBsSco as purified was assayed using the Cu(I) chelator BCA according to the method of Brenner and Harris (*18*). Crystallization was carried out using the hanging drop method at room temperature. The drop consisted of 1.5 μL of 8 mg/mL protein in PBS[2] buffer at pH 7.4 or Tris HCl at pH 7.4 mixed with 1.5 μL of a reservoir solution containing 8.5% polyethylene glycol 5K monomethyl ether, 3.5% $CdCl_2$, 0.2 M $CaCl_2$, and 0.1 M MES at pH 6.5. Cocrystallization was performed with Cu(I) or Cu(II), ranging in final concentration from 0.5 to 25 mM, using Bis-Tris propane buffer from pH 6.5 to 8.5, with or without 2 mM DTT, under an argon atmosphere. Bis-Tris propane was the only common buffer at our disposal in which copper remained soluble in the mixture. Crystals of a size suitable for X-ray structural analysis were obtained in ∼5 days. We also attempted to soak sBsSco crystals with 25 mM Cu(I) or 20 mM Cu(II) and 5 mM DTT or TCEP under the same crystallization conditions for 2, 4, 12, and 54 h. The expression and purification of His-BsSco from *B. subtilis* plasma membranes have been described previously (*15*).

Gel Filtration Chromatography with Multiangle Light Scattering. sBsSco was concentrated to 9 mg/mL by ultrafiltration, degassed, and loaded (500:L) onto a Sephacryl S-200 (Amersham) column (104 cm × 0.7 cm). The S-200 column was equilibrated in degassed PBS (pH 7.4) supplemented with 0.01% (v/v) Tween 20. The eluate was filtered through a 0.22 μm filter (Millipore) and passed on-line to an absorbance monitor (LC-75, Perkin-Elmer) set at 280 nm and then to a DAWN-DSP multiangle laser light scattering detector (Wyatt Technology). The laser light scattered at 15, 26, 35, 43, 52, 60, 69, 80, 90, 100, 111, 121, 132, 142, 152, and 163° angles was collected every 4.0 s. Data collection and analysis were performed using the Astra software

[2] Abbreviations: BCA, bicinchoninic acid; DTDP, 4,4′-dithiodipyridine; DTT, dithiothreitol; PBS, phosphate-buffered saline (10 mM Na_2HPO_4, 2.7 mM KCl, 137 mM NaCl, and 2 mM KH_2PO_4); TCEP, tris(2-carboxyethyl)phosphine hydrochloride; GdnHCl, guanidinium hydrochloride, rmsd; root-mean-square deviation.

package included with the laser light scattering system (Wyatt Technology). The weight-averaged molar mass (M_w) was calculated by regression analysis of the Debye plot according to the method of Zimm (*19, 20*). The value for the protein concentration used in this calculation was determined by absorption at 280 nm using an extinction coefficient of 19 180 M^{-1} cm^{-1}.

Assessment of BsSco Sulfhydryl Residues. The free thiol content of BsSco was determined using the spectrophotometric DTDP assay (*21*). Sufficient buffer [25 mM sodium phosphate (pH 7.0)] was added to both sides of a split cuvette to record a buffer blank spectrum. An aliquot of BsSco (final concentration of 2−10 μM) was added to one side of the split cuvette and the spectrum of the protein recorded. An aliquot of stock DTDP (final concentration of 200 μM) was added to the other side of the split cuvette to maintain equal volumes between the two sides, and spectra were recorded as a function of time to obtain a basal rate of hydrolysis of DTDP. Following this incubation period, the contents of the two sides of the cuvette were mixed. The spectrum obtained just before mixing was subtracted from that obtained just after mixing. The intensity of the absorption band at 324 nm produced by the product 4-thiopyridone was used to calculate the concentration of reactive thiols. The molar absorptivity of 4-thiopyridone [i.e., $\epsilon_{(324)}$] determined under the same conditions using known cysteine concentrations is 18 992 ± 341 M^{-1} cm^{-1}. The cysteine content was determined on sBsSco as isolated, on sBsSco treated with thiol reductants, on the guanidinium HCl-denatured sBsSco, treated and not treated with reductant, on sBsScoHA treated and not treated with reductant, and on His-BsSco.

BsSco was treated with either DTT or TCEP to reduce any disulfide bonds. TCEP reduction was carried out in one of two ways, with stoichiometric amounts of TCEP, or with the reductant in large excess. In the case of stoichiometric reduction, BsSco was incubated with TCEP at a concentration twice that of BsSco for 30 min at room temperature. In experiments in which the reductant was in large excess, BsSco was incubated with 1−2 mM TCEP, or 1−2 mM DTT, for 2−12 h at room temperature. The excess reducing agent was removed by gel filtration on G-25 superfine resin. Denatured BsSco was prepared by incubation of the protein in PBS with 6 M guanidinium hydrochloride for 1 h at room temperature prior to determination of free thiol content.

Mass Spectrometry Analysis. A stock solution of sBsSco at 1 mg/mL (i.e., 50.7 μM) was dialyzed into 10 mM ammonium bicarbonate, diluted to 3 pmol/μL in 50% (v/v) acetonitrile and 0.2% (v/v) formic acid, and sprayed using a syringe pump at a rate of 0.5 μL/min. Mass spectroscopic analysis was carried out on a Q-Tof *Ultima* GLOBAL (Waters Corp.) mass spectrometer fitted with a nano Z spray source. The instrument was calibrated over the mass range of *m*/*z* 70−1400, using the collision-induced dissociation spectra of Glu-fibrinopeptide B, with a polynomial fit of 1. Data were acquired over the range of *m*/*z* 500−3000 with a 2.4 s integration time. Summed spectra were background subtracted, smoothed, and centroided. The resulting spectra were analyzed using the component option in Masslynx 4 (Waters Corp.) to determine the charge state of each ion in the series. The Transform algorithm was used to display the *m*/*z* spectrum on a true molecular mass axis.

Circular Dichroism Spectroscopy. CD spectra were recorded at room temperature on an OLIS RSM CD spectrophotometer. Spectra were recorded from 260 to 177.5 nm in either a 0.1 or 0.01 cm path length cell (Hellma) using concentrations of BsSco ranging from 5 to 100 μM (i.e., from ∼0.1 to 2 mg/mL) in a buffer of 10 mM sodium phosphate (pH 7.0). The protein concentration was determined by the sample's absorption at 280 nm and the extinction coefficient given above. Deconvolution of the secondary structural content was carried out with CDNN (*22*) using the 23-spectrum basis set.

Diffraction Data Collection and Processing. Crystals were transferred to precipitant solution containing 25% glycerol and flash-frozen in liquid nitrogen. The crystals belong to space group $P3_221$, with the following unit cell dimensions: $a = b = 68$ Å and $c = 191$ Å. The asymmetric unit contains two sBsSco molecules, and the solvent content is estimated to be 60.3%. X-ray diffraction data were collected at beamline X12B of the Brookhaven National Laboratory (Upton, NY) at a wavelength of 0.97960 Å for single anomalous dispersion (SAD) phasing. Measured data were integrated, scaled, and merged using DENZO/SCALEPACK (*23*).

Phasing Calculations and Structure Refinement. The selenium positions were determined using SOLVE (*24*), and after density modification using RESOLVE (*25*), an initial electron density map was calculated at 2.0 Å. The map allowed unambiguous tracing of most parts of the molecules, based on which two molecules in the asymmetric unit were built into the electron density map using Xfit (*26*). High-resolution data (1.7 Å) were then used for further cycles of model building and refinement. The model was refined using RAFMAC (*27*) and CNS packages (*28*). Throughout the refinement process, 5% of the reflections were excluded to monitor R_{free}. Several cycles of refinement resulted in a final R factor of 23.8% and a final R_{free} of 28.9%. The structure was well-defined in the final electron density map with the exception of N-terminal residues Gly1 and Ser2 in both molecules, and Glu130 in molecule A due to their weak electron densities. In the course of refinement, we observed that the $F_o - F_c$ difference electron densities in several localities were too strong to assign as water molecules. They may result from ions included in the crystallization solution. The negatively charged environment suggests that they are probably cations. Our crystallization solution contained two such candidates, calcium ions and cadmium ions. In accordance with the levels of the difference density, we included 14 calcium ions and 5 cadmium ions in the refinement. The final average temperature factors for the calcium ions and cadmium ions are 28.44 and 36.71, respectively. There are two molecules in the asymmetric unit. The final crystallographic dimer includes 343 amino acid residues of the 348 total, together with 390 water molecules, 14 calcium ions, and 5 cadmium ions. A Ramachandran plot generated with PROCHECK (*29*) shows that the final model exhibits good geometry with 90% of the residues in the most favored regions. There are three residues, Gln4, Ile5, and Lys6, located at the N-terminus that are clear outliers. This is not surprising given that the N-terminus is highly flexible and the electron density for these residues is much less well-defined. Detailed statistics are listed in Table 1. Since there is very little difference between the native protein structure

Table 1: Analysis of Secondary Structure (%) by UV Circular Dichroism of Various Forms of BsSco[a]

	sBsSco	reductant-treated sBsSco	sBsScoHA mutant	His-BsSco
α-helix	26.0 ± 1.9	28.3	22.3	30.2
antiparallel β-sheet	16.0 ± 1.7	16.5	19.9	12.8
parallel β-sheet	6.2 ± 0.15	6.4	5.9	8.8
β-turn	16.5 ± 0.45	15.9	17.3	18.0
random coil	39.0 ± 0.96	40.3	38.2	31.0

[a] The values for sBsSco were determined on four different samples, and the reported values are the means and standard deviations. The values for the other forms of BsSco are from a single spectral measurement.

at lower resolution (2.5 Å, data not shown) and the Se-Met-labeled protein structure (1.7 Å), in the discussion below the Se-Met structure will be used unless otherwise stated. Figures were generated using MOLSCRIPT (*30*) and RASTER3D (*31*).

RESULTS AND DISCUSSION

Oligomerization and Redox Status of Purified sBsSco. The SDS−PAGE profile of a sample of purified sBsSco from a typical preparation shows a single band with an apparent molecular mass of 23.2 kDa (Figure 1A). Purified sBsSco was subjected to gel filtration chromatography on Sephacryl S-200 coupled to multiangle light scattering for characterization of its molar mass and oligomerization state. The elution profile (Figure 1B) detected by light scattering reveals two high-molecular mass species centered at ∼30 and ∼40 mL with molar masses of 4.77×10^6 and 1.66×10^6, respectively. These high-molecular mass species, presumably aggregated forms of sBsSco, make little contribution to the overall protein content. The vast majority of the protein, 91.5% in the sample in Figure 1, elutes in the third peak centered at 80 mL with a weight-average molar mass of 19 970 ± 550 g/mol. The poly-dispersity index of the major protein band is 1.00 ± 0.063, indicating that this species is homogeneous. The molar mass determined as described above agrees very well with the value of 19 721.13 ± 0.18 obtained by mass spectrometry and the molecular mass of 19 724.1 Da calculated from the primary sequence, and allows us to conclude that more than 90% of sBsSco is in a monomeric state.

The redox status of the conserved pair of cysteine residues in sBsSco was determined by their reactivity with the reagent DTDP. In the protein as isolated, the cysteines are largely nonreactive with DTDP and give a value for the number of cysteines of 0.136 ± 0.11 mol of cysteine per mole of sBsSco. The cysteine reactivity is unchanged when sBsSco is denatured in 6 M GdnHCl, indicating that the low value for the number of cysteines is not due to their inaccessibility in the folded protein. When sBsSco is treated with either of the thiol reductants, TCEP or DTT, nearly two cysteines (1.96 ± 0.23) per mole of sBsSco are observed. Once sBsSco is reduced, its thiol content is stable and returns to basal levels with a half-life of 35 h when incubated in air at room temperature. In addition, the mass as determined by ES-MS of reductant-treated sBsSco increases to 19 723.35 ± 0.35 Da, an increase of approximately 2 Da relative to sBsSco as isolated. The same 2 Da change is observed upon reduction

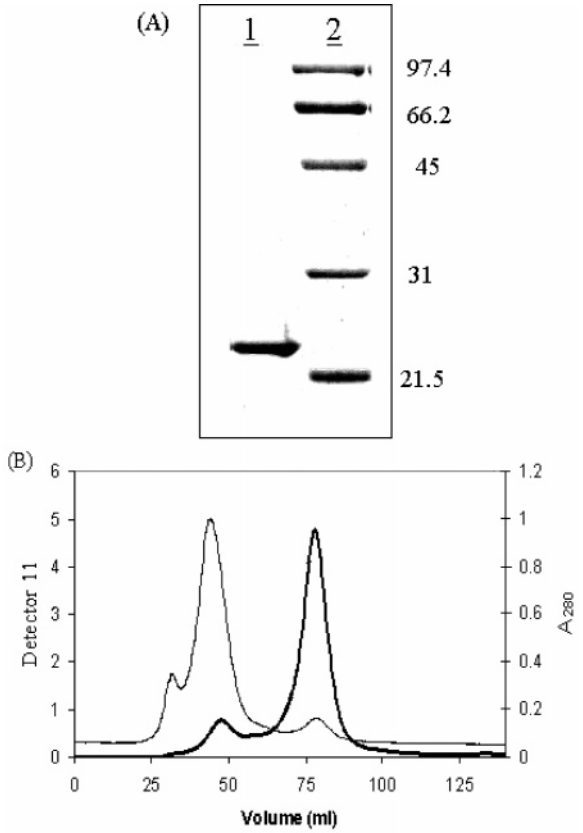

FIGURE 1: Molecular mass and oligomerization state of sBsSco. (A) SDS−PAGE of purified BsSco (15%, stained with Coomassie Blue). Lane 1 contained 2 μg of purified sBsSco. Lane 2 contained a sample of low-molecular mass protein standards from Bio-Rad. The molecular mass of soluble sBsSco was determined from a semilog plot of the migration position of the standards vs their molecular masses. The molecular masses for the standard proteins are indicated at the right. (B) Gel filtration of sBsSco over S-200 Sephacryl equilibrated in PBS (pH 7.4) with 0.01% Tween 20. The thin line shows laser light scattered by sBsSco at detector 11, which is at an angle of 90° with respect to the incident light. The thick line is the absorption of the sample at 280 nm (A_{280}).

of the mutant sBsScoHA from a mass of 19 655.10 ± 0.26 to 19 657.17 ± 0.36 Da. These data along with the monomeric form of sBsSco lead us to conclude that the two conserved cysteine residues are in the form of an intramolecular disulfide in the vast majority of the protein as isolated. In addition, His-BsSco exhibits a similar pattern in that the protein as isolated reveals no free sulfhydryls under native or denaturing conditions, but two sulfhydryls per BsSco can be regenerated by incubation of the native protein with a reductant. In addition, our mass determinations are consistent with the nondetectable levels of copper that we find for both sBsSco and sBsScoHA, as isolated. In contrast, yeast mitochondrial Sco1 has been reported to be purified with 1 equiv of Cu(I) (*32*). This difference may reflect an inherent difference in the affinity of Sco for copper from the two different sources, or that our isolation conditions have led to dissociation of a copper−Sco complex.

Estimation of the Secondary Structure of BsSco. The far-UV CD spectrum of sBsSco shows double minima at 208 and 222 nm and a positive peak at 193 nm characteristic of significant α-helical secondary structure (Figure 2). This spectral form was constant over a period of storage of 18 days at 4 °C, indicating that sBsSco is highly stable. Using the secondary structure analysis program CDNN (*20*), the

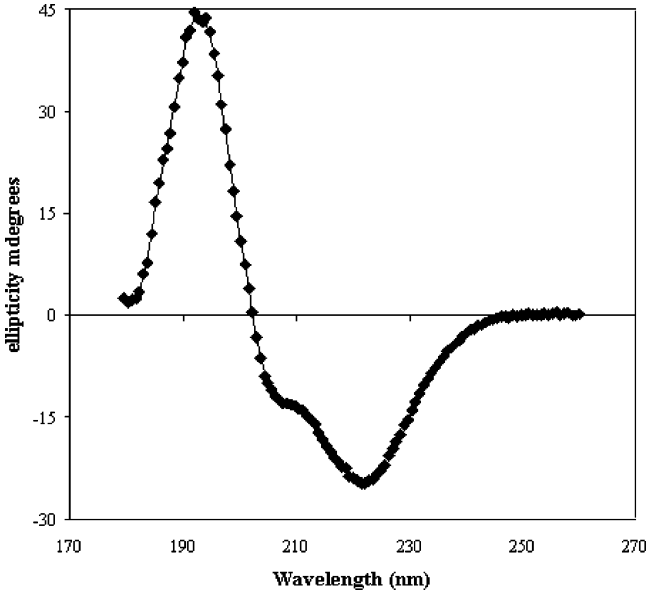

FIGURE 2: Circular dichroism spectrum of sBsSco in the ultraviolet region. The protein was dissolved in 10 mM sodium phosphate (pH 7.0) at a concentration of 0.452 mg/mL. The CD spectra were measured in a 0.1 cm path length cell; the data are the average of eight scans, and the line through the data was generated with nine-point smoothing.

Table 2: Data Collection and Refinement Statistics

	Se-Met-labeled protein	His135Ala mutant
resolution (Å)	50−1.7	50−2.4
total no. of reflections	1001140	191875
no. of unique reflections	108990	21269
R_{sym}	0.082	0.084
completeness (%)	96.2	92
$\langle I/\sigma \rangle$	16.3	9.5
SAD phasing statistics		
no. of heavy atom sites	3	
resolution (Å)	50−2.0	
FOM	0.42	
refinement		
resolution range (Å)	50−1.7	50−2.4
no. of reflections	57557	14832
R (R_{free})	23.8 (28.9)	24.0 (31.8)
no. of protein atoms	2719	2719
no. of divalent ions	19	19
no. of water atoms	390	0
rmsd for bond lengths (Å)	0.006	0.009
rmsd for bond angles (deg)	1.19	1.47

percentage of amino acid residues in a α-helical conformation is estimated to be 26%. This is in good agreement with the number of residues (i.e., 27%) that are in an α-helical conformation in the crystal structure of sBsSso (see below). The full analysis is shown in Table 1 and compared to values obtained for reduced sBsSco, sBsScoHA, and His-BsSco. Although there are small differences between the different forms of BsSco, they retain a very similar complement of secondary structural elements. The native detergent-solubilized version of BsSco is similar to its soluble counterpart, indicating that the structure of sBsSco is a good model of the lipid-bound native protein. However, the possibility that the differences observed between soluble and lipidated versions of BsSco affect the protein's reactivity and reflect a role for membrane anchoring in Sco's functional status must be further explored. The secondary structure appears to be largely unchanged when oxidized sBsSco is reduced

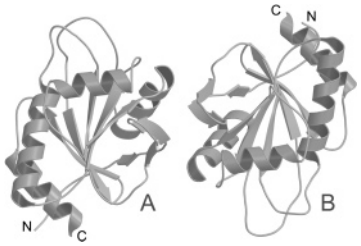

FIGURE 3: Overall structure of two sBsSco molecules, labeled molecules A and B, in the asymmetric unit.

(Table 1) or in the mutant sBsScoHA. Neither the redox state of the two cysteine residues nor the change of histidine 135 to alanine is coupled to large-scale changes in sBsSco's secondary structure. This view is consistent with the limited and local structural changes observed near the active site cysteines for reduced and oxidized *E. coli* thioredoxin (*33*). However, for sBsSco to bind copper with the two cysteines and His135 as inner sphere ligands, a significant conformational change is required (see below).

Overall Crystal Structure. There are two molecules in the asymmetric unit, although sBsSco is a monomer in solution. A single molecule of sBsSco contains four α-helices and eight β-strands (Figure 3). The overall structure of the molecule contains a typical thioredoxin-like fold, despite a relatively low level of sequence identity with other thioredoxin family members (∼17%), which includes a central β-sheet that is made up of β4, β5, β7, and β8. Three flanking α-helices correspond to α1, α3, and α4. There are, however, a number of significant differences. For example, in sBsSco, there is an α-helix (α2) near loop 3 and a β-strand (β6) forms a parallel β-sheet with β5 and is inserted between β5 and β2, which are not seen in thioredoxin (*34*). Three β-strands (β1−β3) and a 3_{10}-helix are present at the N-terminus. The short β2 and β3 strands also form a hairpin.

The backbone superimposition of the sBsSco crystal structure of molecule A (molecule A of the crystallographic dimer illustrated in Figure 3 will be used for discussion from now on unless otherwise stated) and the NMR structures (*17*) show that the overall backbone root-mean-square deviation (rmsd) is 1.97 Å. Apart from the flexible N-terminus (rmsd = 8.8 Å) and the C-terminus (rmsd = 18.45 Å), the most significant difference between the crystal and NMR structures is in the loop 3 region (residues 44−50) and loop 8 region (residues 126−136). The values of the average rmsd for these two regions are 2.91 and 7.36 Å, respectively.

Although the overall structure of the two crystallographically independent molecules is nearly identical (rmsd = 0.14 Å), there are several large local structural differences. The rmsd between loop 8 (residues 126−136) of molecule A and of molecule B is 4.66 Å. The temperature *B*-factor of loop 8 is 53.56, as compared to the average *B*-factor of 30.81 for molecule A and 31.23 for molecule B. The conserved His135, which is a potential copper binding residue (*8*), is located in this loop, where the electron density map is weak. Taken together, these observations indicate that His135-containing loop 8 is very flexible. Loop 3 (residues 44−50) of molecule A and loop 3 of molecule B also exhibit differences, although much less than loop 8. The rmsd of loop3 between the two molecules is 1.56 Å. The *B*-factor (49.40) is also higher than the protein average. Significantly, the conserved Cys45 and Cys49 residues of the CXXXCP

motif are located in this loop. These two loops, loop 8 and loop 3, are both implicated in copper binding, and interestingly, both clearly exhibit conformational plasticity in the structure.

Copper Binding. It has been shown that BsSco is involved in the assembly of the Cu_A center in cytochrome *c* oxidase and may play a role in the transfer of copper to this site. Mutants of BsSco, in which each of the cysteines has been changed to serine or His135 to alanine and expressed in a BsSco-null strain of *B. subtilis*, are unable to restore assembly of cytochrome *c* oxidase (*13*). It has been proposed that the CXXXCP motif and His135 are involved in copper binding (*3*, *8*, *35*). As previously mentioned, the presumptive copper binding residues Cys45 and Cys49 are located in loop 3 between α1 and β4. In the various native and mutant structures and crystallographically independent molecules, the side chain conformations of the two Cys residues are different to varying degrees. In the reduced, or non-disulfide-bonded structure (such as the 1.7 Å Se-Met structure), the thiol group of Cys45 in molecule B is exposed to the solvent while the side chain of Cys49 is encompassed in the CXXXCP loop. In other words, the two groups do not point at each other and the distance between the two S atoms is 7.84 Å. In comparison, the thiol groups of the two cysteines in molecule A are both encompassed in the loop, with an inter-S distance of 3.44 Å. The side chains in molecule A, although closer, still do not point at each other in a linear fashion, and therefore, a disulfide bridge is not formed. If copper were to be coordinated by the two Cys residues, it would not be possible to have copper bound in a linear manner as demonstrated for the structure of CueR, which reveals linear Cu^+ dithiolate coordination by two conserved cysteines (*36*), because the distance is too short. Copper binding to molecule A would require the loop to expand outward a great deal.

We have made extensive attempts, via cocrystallization and crystal soaking, using a range of concentrations of Cu(I) or Cu(II) with or without reducing agents, different buffers, various pH's (6.2 to 8.5), variation of the soaking time (from 2 to 54 h). In addition, cocrystallization for reduced sBsSco has been set up with argon-equilibrated samples, and the manipulations were carried out in an argon atmosphere. These precautions against exposure to oxygen together with the stability of the reduced protein ensure that reduced sBsSco has not undergone nonspecific oxidation during the crystallization process. Unfortunately, after determination of more than 20 structures, we have thus far not found any copper ion in, or beyond the CXXXCP motif. As discussed above, His135 is located in loop 8 that is parallel to loop 3 where the two cysteines are present. The nearest distance between His135 and Cys45 is ~14.1 Å, and between His135 and Cys49 is ~16.1 Å, in molecule A. The distance between His135 and the two cysteines in molecule B is slightly shorter. The distances are ~10.9 Å between His135 and Cys45 and ~12.5 Å between His135 and Cys49. Clearly, if these three residues are to coordinate copper, a large conformational change is necessary (Figure 6). Both loop 3 and loop 8 are flexible which is evident from their weak electron density and relatively high *B*-factors. These two loops show the greatest variation in structures between the crystallographically independent molecules. This is perhaps not by coincidence, since conformational freedom would be required for either copper binding or other functions (see below).

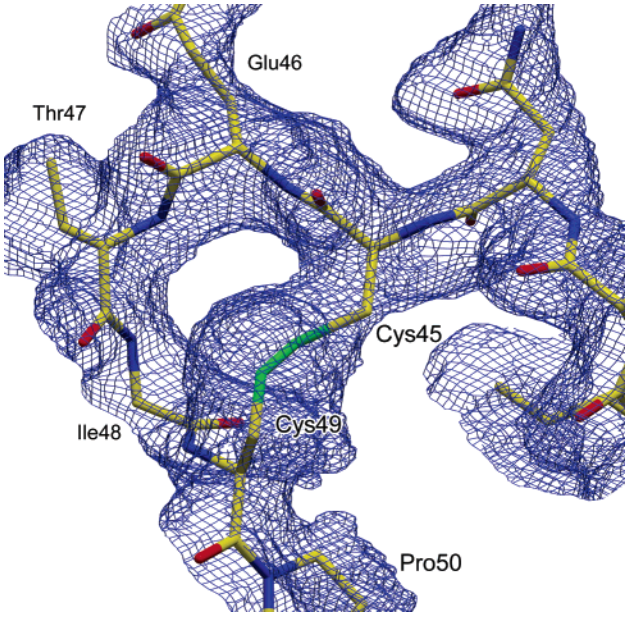

FIGURE 4: Electron density of the non-disulfide-bonded CXXXCP motif in native sBsSco.

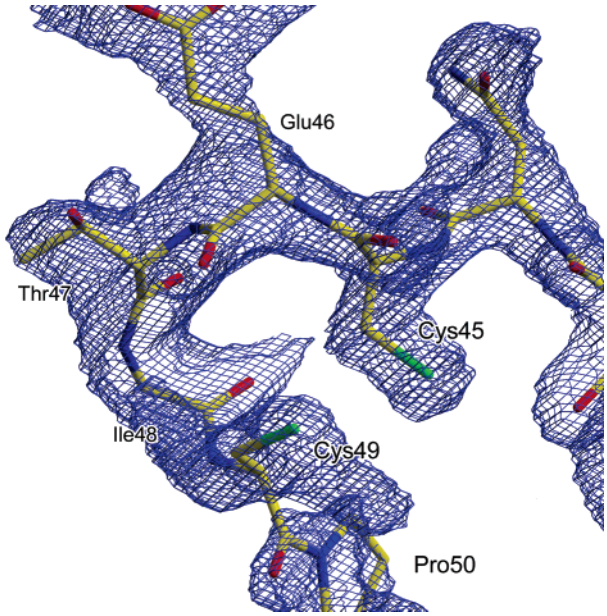

FIGURE 5: Electron density of the disulfide-bonded CXXXCP motif in the His135Ala mutant.

Disulfide Switch. In some structures of copper cocrystals or copper-soaked crystals, a disulfide bridge is observed between Cys45 and Cys49 in molecule A but not in molecule B (Figures 4 and 5). The conditions under which the crystals were obtained vary widely, for example, with or without reducing agents, different buffer and pH, variation of soaking time, and cocrystallization in argon atmosphere (*37*). Furthermore, the His135Ala mutant structure shows that there are disulfide bonds in both crystallographically independent molecules. At this point, it is not clear to us, however, why disulfide bridges form in some crystals but not in others, in molecule A, but not in molecule B, or in both molecules. There seems to be only a small energy barrier separating

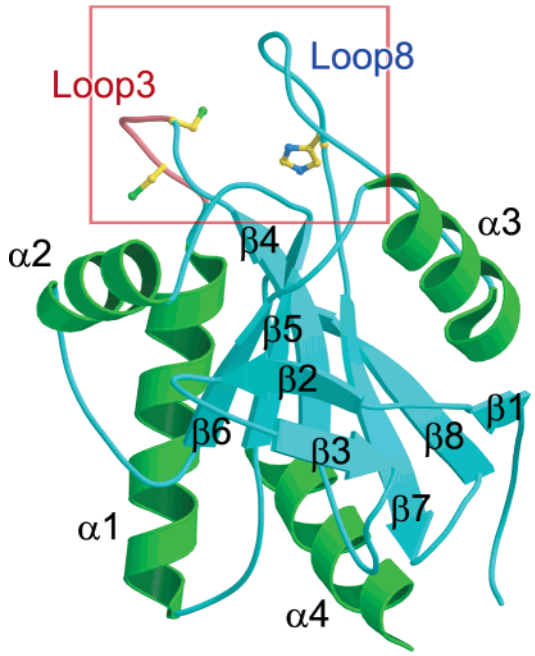

FIGURE 6: Ribbon representation of sBsSco showing the secondary structure elements and CXXXCP motif (pink) with two cysteines. In the highlighted box, three putative copper binding residues are illustrated.

FIGURE 7: Backbone superposition of sBsSco molecule A and oxidoreductase from *M. tuberculosis* with the two key cysteines highlighted. sBsSco is colored light brown, and side chains are colored red. Oxidoreductase is colored green, and side chains are colored blue.

the two conformations, disulfide-bonded and non-disulfide-bonded. Subtle changes in crystallization and/or soaking solutions appear to be able to readily trigger bond formation or breakage. In light of the fact that disulfide bond formation and breakage are hallmarks of the redox activity of thioredoxin family members (*38*−*40*) and the overall structure homology, we therefore suggest that an important function of BsSco is its redox activity, which has not been observed directly until now. We envisage that BsSco may be able to carry out disulfide exchange with the target protein, subunit II of cytochrome *c* oxidase, which contains the Cu_A center. More specifically, the disulfide switch in BsSco could facilitate the assembly of the Cu_A center in cytochrome *c* oxidase via a redox reaction, ensuring the appropriate redox state of the protein partner. The cysteine-containing loop 3 is situated on the surface, is flexible, and projects outward, which are all appropriate attributes for interacting with other protein(s). It is possible that the loop could insert itself into the vicinity of the Cu_A center, not only delivering copper but also carrying out redox activity by disulfide exchange. In this view, His135 of loop 8 would play a crucial role in protein target recognition and docking, or in modulating the reactivity of the key cysteine pair. Such a role for His135 would account for its conservation in *B. subtilis*, yeast, and human forms of Sco.

Comparison between the Structures of BsSco and Thioredoxin-like Proteins. We searched for structural homologues of BsSco (*41*) and identified several proteins that share structural homology with BsSco. These are Mtb DsbE (*Mycobacterium tuberculosis* oxidoreductase) (*42*) (rmsd = 2.75 Å), TryP (tryparedoxin peroxidase) (*43*) (rmsd = 2.82 Å), HBP23 (2-Cys peroxiredoxin heme-binding protein 23) (*44*) (rmsd = 2.8 Å), and TryX (tryparedoxin) (*45*) (rmsd = 2.9 Å), which all share a thioredoxin-like fold. However, the level of sequence identity is less than 17% between BsSco and these structural homologues. In these homologues, two functionally essential cysteines are positioned far from each other in the sequence and have two Val-Cys-Pro motifs in TryP and HBP23. Mtb DsbE and TryX have an active CXXC motif. BsSco is the only thioredoxin-like protein that has a three-residue insertion between the two Cys residues. Although the core of the thioredoxin-like fold is similar in all structures, there are some interesting differences in the position of key cysteines and their vicinity. TryP and HBP23 are both 2-Cys peroxiredoxins in which Cys52 is positioned at the end of an α-helix near the monomer−monomer interface and Cys173 is located in the flexible C-terminus directed toward the solvent. Cys52 from one monomer and Cys173 from another monomer form the active site. TryX and Mtb DsbE have CXXC motifs, both of which are positioned in a redox active site. One cysteine is located at an end of an α-helix, and the other is in the preceding short loop region. The disulfide bonds or thiolate groups of the pair of cysteines in the active site are only partially exposed. In comparison, the two Cys residues in sBsSco are located in a protruding loop that is exposed to the solvent. The environment of this putative active site is unusually acidic due to residues Glu46, Glu128, Glu130, and Asp131. Phe42, Pro50, Try94, and Phe90 form a hydrophobic groove running alongside the pair of cysteines. The hydrophobic characteristics would help BsSco interact with another protein (*46*). These features are not observed in other thioredoxin-like proteins. The cysteines of the CXXC motif of TryX and Mtb DsbE are in an approximately similar location as the CXXXCP motif of sBsSco. However, CXXXCP in sBsSco loop3 protrudes toward the solvent much more than TryX and Mtb DsbE (Figure 7), supporting the notion that the Cys pair of BsSco is perhaps more flexible than its counterparts in TryX and Mtb DsbE which leads to the dual function of copper delivery and redox activity.

ACKNOWLEDGMENT

We thank Brookhaven National Laboratory for the use of beamline X12B at National Synchrotron Light Source, particularly Annie Heroux who helped with X-ray data collection. We also thank Diann Andrews for help with fusion constructs of BsSco, Daniel Lee for help with figures, and Melanie Adams for help with model building.

REFERENCES

1. Brzezinski, P., and Larsson, G. (2003) Redox-driven proton pumping by heme-copper oxidases, *Biochim. Biophys. Acta 1605*, 1−13.
2. Michel, H., Behr, J., Harrenga, A., and Kannt, A. (1998) Cytochrome *c* oxidase: Structure and spectroscopy, *Annu. Rev. Biophys. Biomol. Struct. 27*, 329−356.
3. Carr, H. S., and Winge, D. R. (2003) Assembly of cytochrome *c* oxidase within the mitochondrion, *Acc. Chem. Res. 36*, 309−316.
4. Glerum, D. M., Shtanko, A., and Tzagoloff, A. (1996) SCO1 and SCO2 act as high copy suppressors of a mitochondrial copper recruitment defect in *Saccharomyces cerevisiae*, *J. Biol. Chem. 271*, 20531−20535.
5. McEwan, A. G., Lewin, A., Davy, S. L., Boetzel, R., Leech, A., Walker, D., Wood, T., and Moore, G. R. (2002) PrrC from *Rhodobacter sphaeroides*, a homologue of eukaryotic Sco proteins, is a copper-binding protein and may have a thiol-disulfide oxidoreductase activity, *FEBS Lett. 518*, 10−16.
6. Papadopoulou, L. C., Sue, C. M., Davidson, M. M., Tanji, K., Nishino, I., Sadlock, J. E., Krishna, S., Walker, W., Selby, J., Glerum, D. M., Coster, R. V., Lyon, G., Scalais, E., Lebel, R., Kaplan, P., Shanske, S., De, V. D., Bonilla, E., Hirano, M., DiMauro, S., and Schon, E. A. (1999) Fatal infantile cardioencephalomyopathy with COX deficiency and mutations in SCO2, a COX assembly gene, *Nat. Genet. 23*, 333−337.
7. Schulze, M., and Rodel, G. (1989) Accumulation of the cytochrome *c* oxidase subunits I and II in yeast requires a mitochondrial membrane-associated protein, encoded by the nuclear SCO1 gene, *Mol. Gen. Genet. 216*, 37−43.
8. Nittis, T., George, G. N., and Winge, D. R. (2001) Yeast Sco1, a protein essential for cytochrome *c* oxidase function is a Cu(I)-binding protein, *J. Biol. Chem. 276*, 42520−42526.
9. Chinenov, Y. V. (2000) Cytochrome *c* oxidase assembly factors with a thioredoxin fold are conserved among prokaryotes and eukaryotes, *J. Mol. Med. 78*, 239−242.
10. Glerum, D. M., Shtanko, A., and Tzagoloff, A. (1996) Characterization of COX17, a yeast gene involved in copper metabolism and assembly of cytochrome oxidase, *J. Biol. Chem. 271*, 14504−14509.
11. Beers, J., Glerum, D. M., and Tzagoloff, A. (1997) Purification, characterization, and localization of yeast Cox17p, a mitochondrial copper shuttle, *J. Biol. Chem. 272*, 33191−33196.
12. Seib, K. L., Jennings, M. P., and McEwan, A. G. (2003) A Sco homologue plays a role in defence against oxidative stress in pathogenic *Neisseria*, *FEBS Lett. 546*, 411−415.
13. Mattatall, N. R., Jazairi, J., and Hill, B. C. (2000) Characterization of YpmQ, an accessory protein required for the expression of cytochrome *c* oxidase in *Bacillus subtilis*, *J. Biol. Chem. 275*, 28802−28809.
14. Tjalsma, H., Kontinen, V. P., Pragai, Z., Wu, H., Meima, R., Venema, G., Bron, S., Sarvas, M., and van Dijl, J. M. (1999) The role of lipoprotein processing by signal peptidase II in the Gram-positive eubacterium bacillus subtilis. Signal peptidase II is required for the efficient secretion of alpha-amylase, a non-lipoprotein, *J. Biol. Chem. 274*, 1698−1707.
15. Andrews, D., Rattenbury, J., Anand, V., Mattatall, N. R., and Hill, B. C. (2004) Expression, purification, and characterization of BsSco, an accessory protein involved in the assembly of cytochrome *c* oxidase in *Bacillus subtilis*, *Protein Expression Purif. 33*, 57−65.
16. Imriskova-Sosova, I., Ye, Q., Hill, B. C., and Jia, Z. (2003) Purification, crystallization and preliminary X-ray analysis of a Sco1-like protein from *Bacillus subtilis*, a copper-binding protein involved in the assembly of cytochrome *c* oxidase, *Acta Crystallogr. D59*, 1299−1301.
17. Balatri, E., Banci, L., Bertini, I., Cantini, F., and Ciofi-Baffoni, S. (2003) Solution structure of Sco1: A thioredoxin-like protein involved in cytochrome *c* oxidase assembly, *Structure 11*, 1431−1443.
18. Brenner, A. J., and Harris, E. D. (1995) A quantitative test for copper using bicinchoninic acid, *Anal. Biochem. 226*, 80−84.
19. Wyatt, P. J. (1993) Light scattering and the absolute characterization of macromolecules, *Anal. Chim. Acta 272*, 1−40.
20. Zimm, B. H. (1948) Apparatus and methods for measurement and interpretation of the angular variation of light scattering: Preliminary results on polystyrene solutions, *J. Chem. Phys. 16*, 1099−1016.
21. Riener, C. K., Kada, G., and Gruber, H. J. (2002) Quick measurement of protein sulfhydryls with Ellman's reagent and with 4,4′-dithiodipyridine, *Anal. Bioanal. Chem. 373*, 266−276.
22. Bohm, G., Muhr, R., and Jaenicke, R. (1992) Quantitative analysis of protein far UV circular dichroism spectra by neural networks, *Protein Eng. 5*, 191−195.
23. Otwinowski, Z., and Minor, W. (1997) Processing of X-ray diffraction data collected in oscillation mode, *Methods Enzymol. 276*, 307−326.
24. Terwilliger, T. C., and Berendzen, J. (1999) Automated MAD and MIR structure solution, *Acta Crystallogr. D55*, 849−861.
25. Terwilliger, T. C. (2003) Statistical density modification using local pattern matching, *Acta Crystallogr. D59*, 1688−1701.
26. McRee, D. E. (1999) XtalView/Xfit: A versatile program for manipulating atomic coordinates and electron density, *J. Struct. Biol. 125*, 156−165.
27. Murshudov, G. N., Vagin, A. A., and Dodson, E. J. (1997) Refinement of Macromolecular Structures by the Maximum-Likelihood Method, *Acta Crystallogr. D53*, 240−255.
28. Brunger, A. T., Adams, P. D., Clore, G. M., DeLano, W. L., Gros, P., Grosse-Kunstleve, R. W., Jiang, J. S., Kuszewski, J., Nilges, M., Pannu, N. S., Read, R. J., Rice, L. M., Simonson, T., and Warren, G. L. (1998) Crystallography & NMR system: A new software suite for macromolecular structure determination, *Acta Crystallogr. D54*, 905−921.
29. Laskowski, R. A., MacArthur, R. W., Moss, D. S., and Thornton, J. M. (1993) PROCHECK: A program to check the stereochemical quality of protein structures, *J. Appl. Crystallogr. 26*, 283−291.
30. Kraulis, P. J. (1991) MOLSCRIPT: A program to produce both detailed and schematic plots of protein structures, *J. Appl. Crystallogr. 24*, 946−950.
31. Merritt, E. A., and Bacon, D. J. (1997) Raster 3D: Photorealistic molecular graphics, *Methods Enzymol. 277*, 505−524.
32. Beers, J., Glerum, D. M., and Tzagoloff, A. (2002) Purification and characterization of yeast Sco1p, a mitochondrial copper protein, *J. Biol. Chem. 277*, 22185−22190.
33. Holmgren, A. (1995) Thioredoxin structure and mechanism: Conformational changes on oxidation of the active-site sulfhydryls to a disulfide, *Structure 3*, 239−243.
34. Martin, J. L. (1995) Thioredoxin: A fold for all reasons, *Structure 3*, 245−250.
35. Rentzsch, A., Krummeck-Weiss, G., Hofer, A., Bartuschka, A., Ostermann, K., and Rodel, G. (1999) Mitochondrial copper metabolism in yeast: Mutational analysis of Sco1p involved in the biogenesis of cytochrome *c* oxidase, *Curr. Genet. 35*, 103−108.
36. Changela, A., Chen, K., Xue, Y., Holschen, J., Outten, C. E., O'Halloran, T. V., and Mondragon, A. (2003) Molecular basis of metal-ion selectivity and zeptomolar sensitivity by CueR, *Science 301*, 1383−1387.
37. Evrard, C., Capron, A., Marchand, C., Clippe, A., Wattiez, R., Soumillion, P., Knoops, B., and Declercq, J. P. (2004) Crystal structure of a dimeric oxidized form of human peroxiredoxin 5, *J. Mol. Biol. 337*, 1079−1090.
38. Kadokura, H., Katzen, F., and Beckwith, J. (2003) Protein disulfide bond formation in prokaryotes, *Annu. Rev. Biochem. 72*, 111−135.
39. Wood, Z. A., Schroder, E., Robin, H. J., and Poole, L. B. (2003) Structure, mechanism and regulation of peroxiredoxins, *Trends Biochem. Sci. 28*, 32−40.
40. Yano, H., Kuroda, S., and Buchanan, B. B. (2002) Disulfide proteome in the analysis of protein function and structure, *Proteomics 2*, 1090−1096.

41. Krissinel, E., and Henrick, K. (2003) Protein structure comparison in 3D based on secondary structure matching (SSM) followed by Cα alignment, scored by a new structural similarity function, *Proc. 5th Intern. Confer. Mol. Struct. Biol.*, 88.
42. Goulding, C. W., Apostol, M. I., Gleiter, S., Parseghian, A., Bardwell, J., Gennaro, M., and Eisenberg, D. (2004) Gram-positive DsbE proteins function differently from Gram-negative DsbE homologs. A structure to function analysis of DsbE from *Mycobacterium tuberculosis*, *J. Biol. Chem. 279*, 3516−3524.
43. Alphey, M. S., Bond, C. S., Tetaud, E., Fairlamb, A. H., and Hunter, W. N. (2000) The structure of reduced tryparedoxin peroxidase reveals a decamer and insight into reactivity of 2Cys-peroxiredoxins, *J. Mol. Biol. 300*, 903−916.
44. Hirotsu, S., Abe, Y., Okada, K., Nagahara, N., Hori, H., Nishino, T., and Hakoshima, T. (1999) Crystal structure of a multifunctional 2-Cys peroxiredoxin heme-binding protein 23 kDa/proliferation-associated gene product, *Proc. Natl. Acad. Sci. U.S.A. 96*, 12333−12338.
45. Alphey, M. S., Gabrielsen, M., Micossi, E., Leonard, G. A., McSweeney, S. M., Ravelli, R. B., Tetaud, E., Fairlamb, A. H., Bond, C. S., and Hunter, W. N. (2003) Tryparedoxins from *Crithidia fasciculata* and *Trypanosoma brucei*: Photoreduction of the redox disulfide using synchrotron radiation and evidence for a conformational switch implicated in function, *J. Biol. Chem. 278*, 25919−25925.
46. Guddat, L. W., Bardwell, J. C., Zander, T., and Martin, J. L. (1997) The uncharged surface features surrounding the active site of *Escherichia coli* DsbA are conserved and are implicated in peptide binding, *Protein Sci. 6*, 1148−1156.

BI0480537